Source apportionment and health risk assessment of PM_{10} bound carbonaceous and elemental species in the central Himalayas

Sakshi Gupta[1,2], Preeti Tiwari[1,2], Priyanka Srivastava[3], Manish Naja[3], Nikki Choudhary[1,2], Narayanasamy Vijayan[1,2], Manoj Kumar[1,2], Sudhir Kumar Sharma[1,2*]

[1] CSIR-National Physical Laboratory, Dr. K. S. Krishnan Road, New Delhi 110012, India.
[2] Academy of Scientific and Innovative Research (AcSIR), Ghaziabad 201002, India
[3] Atmospheric Division, Aryabhata Research Institute of Observational Sciences (ARIES), Nainital 263002, Uttarakhand, India.

Volume 1, Issue 2, March 2024
Received: 6 February, 2024; Accepted: 14 March, 2024
DOI: https://doi.org/10.63015/2e-2418.1.2

**Correspondence author email: sudhircsir@gmail.com*

Abstract: In this extensive investigation, the sources and health risk assessment of carbonaceous aerosols, as well as the elemental compositions (Ca, Al, Fe, S, K, Mg, Pd, B, Mo, Zn, Ag, Nb, Ga, Cl, Ti, Zr, Na, Cr, Cu, Mn, Cs, P, Y, Sb, Ni, Sn, F, Sr, Br, Pm, U, Pb, Th, Br, Rb, and V) of PM_{10}, were conducted throughout January-December 2021 in Nainital, a central Himalayan region of India. The average annual mass concentration of PM_{10} was determined to be 64±6 µg m^{-3}. Carbonaceous aerosols (CAs), comprising OC, EC, WSOC, and SOC, exhibited annual averages of 9.3±0.8 µg m^{-3}, 4.9±0.5 µg m^{-3}, 1.5±0.2 µg m^{-3}, 2.7±0.2 µg m^{-3}, and 2.97±0.45 µg m^{-3}, respectively. The elemental composition featured major contributors such as Ca, Al, Fe, S, and K, alongside trace levels of various elements (Mg, Pd, B, Mo, Zn, Ag, Nb, Ga, Cl, Ti, Zr, Na, and Cr). Positive Matrix Factorization (PMF) identified six primary contributors to PM_{10}, each with varying percentage contributions: crustal/soil/road dust, soil re-suspension, combustion, vehicular emissions, industrial emissions, and biomass burning. The health risk assessment revealed elevated Hazard Quotient (HQ) values for Cr and Mn in children, indicating a non-carcinogenic health risk. Adults exposed to high Cr levels may face potential carcinogenic risks, while elements like Al, Pb, Cu, Zn, and Ni pose no health hazards, aligning with USEPA guidelines.

Keywords: PM_{10}, Carbonaceous aerosols, Elemental composition, Source apportionment, Health risk assessment

1. Introduction: Atmospheric aerosols play a crucial role in shaping regional and global climates, affecting air quality, visibility, the Earth's radiation balance, the hydrological cycle, human well-being, crop production, and ecosystems [1]. Carbonaceous aerosols, composed of organic carbon (OC) and elemental carbon (EC) or black carbon (BC), have significant impacts on human health, radiative forcing, and climate change [2, 3]. In urban areas, carbonaceous aerosols contribute to 20–70% of the total aerosol mass, influencing the solar radiation budget [4,5]. Emissions of carbonaceous aerosols from sources like biomass burning, vehicles, and coal-based industries produce hazardous gases such as carbon monoxide (CO), volatile organic compounds (VOCs), and polycyclic aromatic hydrocarbons (PAHs) [6-11], impacting respiratory and lung health [12]. Carbonaceous aerosols can be emitted directly (primary organic aerosols, POA) or formed indirectly in the atmosphere from VOCs through gas-phase oxidation [11]. The intricate interplay between pollutants, including carbonaceous species and trace elements, has far-reaching implications for environmental quality and public health [3]. The Himalayan ecosystem, including Nainital, faces significant challenges due to various pollutants [13]. Nainital's unique geographical and meteorological characteristics make it an ideal setting for such investigations [14-16]. Understanding the composition and sources of

PM_{10} in this region is crucial for effective air quality management and protecting the local population's well-being [17].

This study utilizes advanced analytical techniques to explore the elemental composition of PM_{10}, uncovering major and trace elements with diverse sources, both natural and anthropogenic [3, 14-16, 18]. Our goal is to identify and characterize the sources of PM_{10} in Nainital, unraveling complex atmospheric processes contributing to pollution levels. Additionally, assessing carbonaceous species within PM_{10} will provide insights into the role of combustion-related emissions, biomass burning, and vehicular activities in shaping the region's air quality [15, 16]. Air masses from the anthropogenically influenced Indo-Gangetic Plain (IGP) region, carrying elevated levels of crop residue burning by-products and industrial emissions, impact the area throughout the year, extending to oceanic regions [15, 19]. Beyond characterizing pollution sources, the study evaluates potential health impacts associated with PM_{10} exposure. Understanding health implications is crucial for developing targeted mitigation measures and promoting sustainable development practices in the region. The findings aim to contribute to scientific understanding of air quality dynamics in the Himalayan region and inform policy interventions prioritizing the well-being of local communities [17]. This comprehensive assessment bridges the gap in our knowledge regarding PM_{10} in the Himalayan region, offering a nuanced understanding of its elemental composition, sources, and health impacts, with Nainital serving as a representative case study.

2. Material & Methods:

2.1. Sampling Site: PM_{10} samples were collected at the Aryabhata Research Institute of Observational Science (ARIES) in the Manora Hills of Nainital, India (29.35°N, 79.45°E, 1958 m above mean sea level) from January to December 2021, excluding monsoon months (July, August, September) due to precipitation. A total of 40 PM_{10} samples were collected over 24 h, twice a week using pre-baked (at 550 °C) Pallflex quartz microfiber filters with a Particle Sampler (Model APM460, manufactured by M/s. Envirotech, India). The samples were preserved in a deep freezer at -20°C until chemical analysis. The sampler's average flow rate stood at 1.2 m^3 min^{-1}, with a flow accuracy of within ±2% of its full scale. Pre- and post-sampling, filters underwent desiccation, and their initial and final weights were determined using a microbalance with a precision of ±10 µg. PM_{10} concentration was assessed via gravimetric means. For detailed information on the sampling process, instrumentation used, and methodology, readers can refer to previous publications [3, 14, 15].

2.2. Chemical Analysis: To investigate carbonaceous aerosols, the study focused on estimating the OC (organic carbon), EC (elemental carbon), and WSOC (water-soluble organic carbon) fractions within the PM_{10} samples. The OC/EC carbon analyzer (DRI 2001A, Atmoslytic Inc., Calabasas, CA, USA) was employed for quantifying OC and EC, utilizing the Interagency Monitoring of Protected Visual Environments (IMPROVE-A) procedure [20]. An area of approximately 0.536 cm^2 on the filter was carefully excised using the appropriate punch and subsequently subjected to duplicate analysis, providing outputs for OC (OC1, OC2, OC3, OC4) and OP (optical pyrolysis), as well as EC (EC1, EC2, and EC3) [21]. Quartz filters, commonly employed for PM collection and carbon content estimation via thermal-optical analysis, pose challenges such as potential gaseous organic absorption and OC volatilization. Addressing these, the relative impact of such artifacts was assessed using QBQ methods (sample is set up with a secondary quartz filter positioned behind either the primary quartz filter or a Teflon filter, aligned in parallel), with blank filter OC/EC values subtracted from sample results [22]. To

determine WSOC in PM_{10} samples, a TOC analyser (Model: Shimadzu TOC-L CPH/CPN, Japan) was utilized, with a punch size of 30 mm diameter (7.065 cm^2) from PM_{10} for the analysis [21, 25]. The estimation of primary organic carbon (POC) and secondary organic carbon (SOC) was carried out using the EC tracer method, a common approach [15, 26]. Both OC and EC are products of fuel combustion, with EC serving as the primary tracer for POC. The ratio of OC to EC in fresh aerosols emitted during combustion, denoted as $(OC/EC)_{min}$, was used, and specific formulas were applied to calculate POC and SOC (Eqn. 1, and 2):

$$POC = [EC] \times ({}^{OC}/_{EC})_{min} \quad (1)$$

$$SOC = OC - POC \quad (2)$$

To conduct elemental analysis encompassing a total of 36 elements (including Ca, Al, Fe, S, K, Mg, Pd, B, Mo, Zn, Ag, Nb, Ga, Cl, Ti, Zr, Na, Cr, Cu, Mn, Cs, P, Y, Sb, Ni, Sn, F, Sr, Br, Pm, U, Pb, Th, Br, Rb, and V) in PM_{10} samples, a Wavelength Dispersive X-ray Fluorescence (WD-XRF) Spectrometer (Rigaku ZSX Primus) was utilized. The spectrometer setup comprised a scintillation counter (SC) for detecting heavy elements and a flow-proportional counter (F-PC) for detecting light elements, alongside a sealed X-ray tube for excitation, an end window, and a Rh-target. Measurements were conducted under vacuum conditions, at a temperature of 36°C, and with a tube rating of 2.4 kW. Various detection methods were employed for different elements: F-PC for Mg, Al, P, S, Cl, K, and Ca; RX25 analyzer crystal for Mg; PET analyzer crystal for Al; Ge analyzer crystal for P, Cl, and S; LiF (200) analyzer crystal for Ca and K; and SC detector along with a LiF (200) analyzer crystal for Ti, Cr, Mn, Fe, and Zn. Blank filters were also subjected to analysis to rectify intensities, ensuring precision with a repeatability error falling within the 5–10% range. Comprehensive details regarding the analytical procedures can be found in Sharma et al [3].

2.3. Source Apportionment and Trajectory Analysis: In this study, the Positive Matrix Factorization (PMF) technique was employed on PM_{10} chemical constituents (OC, EC, WSOC, Ca, Al, Fe, S, K, Mg, B, Mo, Zn, Ga, Cl, Ti, Zr, Na, Cr, Cu, Mn, Ni, and P) to identify the sources influencing PM_{10} concentration, using the US-EPA PMF 5.0. The PMF model involves decomposing a speciated data matrix (X) into factor contribution (C) and profile (P) matrices, along with a residual matrix (e) (Eqn. 3).

$$X = C \times P + e \quad (3)$$

The standard equation-based uncertainty (U) is derived through Eqn. 4, incorporating error fraction (ef), concentration (C), and the method detection limit (MDL) of the species [24].

$$U = \sqrt{(ef \times C)^2 + (0.5 \times MDL)^2} \quad (4)$$

$$U = \frac{5}{6} \times MDL, \qquad C < MDL$$

Evaluation of model fit is based on Q-robust, excluding values with scaled residuals exceeding 4, compared to Q-true. Species with significant residuals indicate poor fitting, and error estimation employs DISP, BS, and BS-DISP methods [16, 28-30].

Air mass backward trajectory analysis was conducted using ARL datasets and the HYSPLIT model, tracing the pathways of PM_{10} from the receptor site at 500 m above ground level (AGL). The TrajStat software was employed to generate and analyses 120 h trajectories [15, 25].

2.4. Health Risk Assessment (HRA): The calculation of the HRA followed criteria recommended by the United States Environmental Protection Agency (USEPA). Utilizing data from the Integrated Risk Information System (IRIS) database, the carcinogenic and non-carcinogenic risks associated with inhalation exposure to PM_{10} elements (Al, Cr, Ni, Pb, Mn, Cu, and Zn) were evaluated. Among all the elements identified only heavy elements assessment was

conducted as per USEPA guidelines. Health risks were quantified through exposure concentration (EC) in terms of lifetime average daily dose, Hazard Quotient (HQ), and Carcinogenic Risk (CR) equations 5-7. The Hazard Quotient (HQ) exceeding 1 indicates potential adverse effects on human health, while CR assesses the additional probability of developing cancer throughout a person's lifetime. Reference values were adopted from USEPA, with acceptable cancer risk levels defined within a recommended range [31-33].

$$EC = \frac{C \times IR \times CF \times EF \times ED}{BW \times AT_n} \quad (5)$$

In the context of the calculation, C represents the concentration of the species (µg m^{-3}). Additionally, IR denotes the air inhalation rate, with values set at 10 m^3 day^{-1} for children and 20 m^3 day^{-1} for adults. The correction factor unit (CF) is defined as 0.001, EF stands for relative exposure frequency measured in days per year, ED represents exposure duration set at 24 years, BW corresponds to body weight (15 Kg for children and 70 Kg for adults), and AT_n signifies the average time (calculated as 70 years × 365 days × 24 h day^{-1}).

$$HQ = \frac{EC}{RFD} \quad (6)$$

The reference exposure dose (RFD) for the human population, expressed in mg m^{-3}, was adopted from USEPA 2015.

$$CR = \frac{C \times ET \times EF \times ED \times IUR}{AT} \quad (7)$$

In this context, ET represents exposure time (12 h/day), and IUR stands for the inhalation unit risk ((µg m^{-3})$^{-1}$) derived from elements in the USEPA IRIS (1995) database.

3. Results & Discussions:

3.1. Concentrations of PM_{10} Constituents: The annual average PM_{10} mass concentration (±SE) was estimated as 64 ± 6 µg m^{-3} in Nainital, closely resembling the National Ambient Air Quality Standards (NAAQS) of 60 µg m^{-3} annually but surpassing the World Health Organization (WHO) limits by fourfold (15 µg m^{-3}) (Table 1). Elevated PM_{10} levels have been associated with adverse health effects, including impaired lung function in children, respiratory issues, asthma exacerbations, and potential risks for adults, such as heart diseases, diabetes, and neurological problems [32, 34]. Previous studies in Nainital indicated an average PM_{10} concentration of 65 ± 41 µg m^{-3} and 67 ± 26 µg m^{-3} respectively that is closely correlated to our study [15, 23]. Hooda et al [24], reported the annual long term PM_{10} concentration at Mukteshwar, situated North-East direction to Nainital (~50 km) was 40 ± 30 µg m^{-3}. Fig. 1 represents the temporal variations of carbonaceous aerosols including OC, EC, WSOC, and SOC.

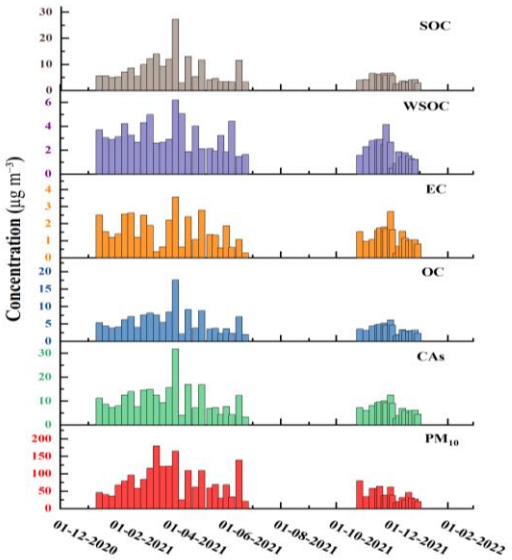

Figure 1. Time series of concentrations (µg m^{-3}) of PM_{10}, and carbonaceous aerosols at Nainital

Also, Table 1 shows the annual average concentrations for the same.

Table 1: Annual average concentrations (±SE) (in µg m^{-3}) of PM_{10} and their chemical constituents at Nainital.

Species	Average (µg m^{-3})	Range (µg m^{-3})
PM_{10}	64±6	16-180
OC	4.90±0.45	1.5-17.6
EC	1.48±0.12	0.3-3.6
WSOC	2.72±0.19	0.5-6.2
CAs	9.32±0.82	2.7-27.4
SOC	2.97±0.45	0.38-3.46
B	0.252±0.024	0.04-0.62
Na	0.106±0.031	0.003-0.944

Mg	0.377±0.081	0.015-2.648
Al	1.498±0.272	0.07-7.99
P	0.042±0.007	0.002-0.170
S	1.303±0.142	0.06-3.91
Cl	0.127±0.033	0.005-1.216
K	1.175±0.152	0.06-4.02
Ca	1.789±0.351	0.089-11.013
Ti	0.110±0.018	0.02-0.50
Cr	0.104±0.010	0.089-0.205
Mn	0.067±0.011	0.03-0.26
Fe	1.479±0.207	0.218-6.020
Ni	0.023±0.003	0.026-0.073
Cu	0.088±0.019	0.029-0.370
Zn	0.231±0.034	0.013-0.835
Ga	0.130±0.032	0.029-0.625
Zr	0.107±0.033	0.013-1.260
Mo	0.238±0.174	0.033-7.174
Br	0.010±0.009	0.03-0.35
Nb	0.165±0.111	0.025-4.031
Ag	0.166±0.076	0.69-2.22
Pb	0.005±0.003	0.089-0.107
Sr	0.013±0.004	0.031-0.106
Y	0.030±0.021	0.04-0.85
F	0.013±0.007	0.137-0.228
Pd	0.254±0.091	0.59-2.34
U	0.006±0.004	0.077-0.106
Sn	0.020±0.018	0.09-0.73
Cs	0.060±0.060	0.068-0.076

The annual average concentrations (±SE) of OC, EC, WSOC, and SOC were determined as 4.90±0.45 μg m^{-3} (range: 1.5-17.6), 1.48±0.12 μg m^{-3} (range: 0.3-3.6), 2.72±0.19 μg m^{-3} (range: 0.5-6.2), and 2.97±0.45 μg m^{-3} (range: 0.38-3.46), respectively. Total carbon (TC=OC+EC) concentration contributed ~10% to PM_{10} (with OC at 7.7% and EC at 2.3%), while SOC contributed around 4.6% to PM_{10}. The fraction of carbonaceous aerosols (CAs) in PM_{10}, calculated as the sum of organic matter (OM=1.6×OC) and EC, accounted for ~14.5% of the PM_{10} load [35]. Elevated levels of OC and EC indicated a notable influence from agricultural waste burning, particularly during rice and wheat harvesting in the north-western region of the Indo-Gangetic Plain, along with the trans-border movement of pollutants to the receptor sites [21, 36].

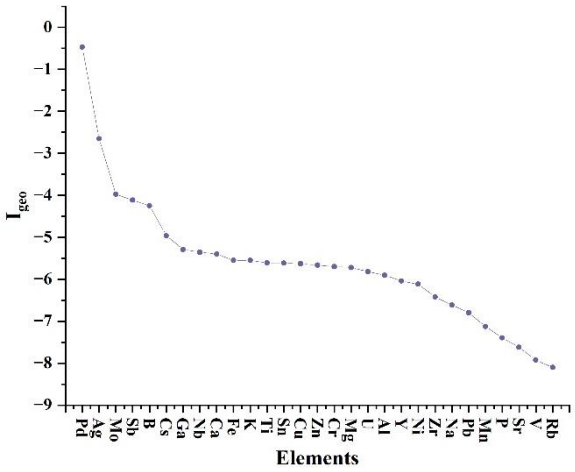

Figure 2: **Geo-accumulation index (I_{geo}) of the elements of PM_{10} over Nainital**

The total elemental composition contributed ~16% to the total PM_{10} mass concentration at the study site. Table 1 illustrates the annual average elemental concentrations, with Ca (1.789 ± 0.351 μg m^{-3}), Al (1.498 ± 0.272 μg m^{-3}), Fe (1.479 ± 0.207 μg m^{-3}), S (1.303 ± 0.142 μg m^{-3}), and K (1.175 ± 0.152 μg m^{-3}) identified as major contributors to PM_{10} concentrations. Elements such as Mg (0.377 ± 0.081 μg m^{-3}), Pd (0.254 ± 0.091 μg m^{-3}), B (0.252 ± 0.024 μg m^{-3}), Mo (0.238 ± 0.174 μg m^{-3}), Zn (0.231 ± 0.034 μg m^{-3}), Ag (0.166 ± 0.076 μg m^{-3}), Nb (0.165 ± 0.111 μg m^{-3}), Ga (0.130 ± 0.032 μg m^{-3}), Cl (0.127 ± 0.033 μg m^{-3}), Ti (0.110 ± 0.018 μg m^{-3}), Zr (0.107 ± 0.033 μg m^{-3}), Na (0.106 ± 0.031 μg m^{-3}), and Cr (0.104 ± 0.010 μg m^{-3}) were detected at trace levels. Other elements, including Cu, Mn, Cs, P, Y, Sb, Ni, Sn, F, Sr, Br, Pm, U, Pb, Th, Fr, Rb, and V, were quantified in the nanogram range (10 ng m^{-3} to 88 ng m^{-3}). The elemental composition of PM_{10} particles was also assessed using the geo-accumulation index (I_{geo}) (Fig. 2). The negative values obtained for all elements indicate the presence of elemental contamination within the study site, suggesting minimal pollution. [60].

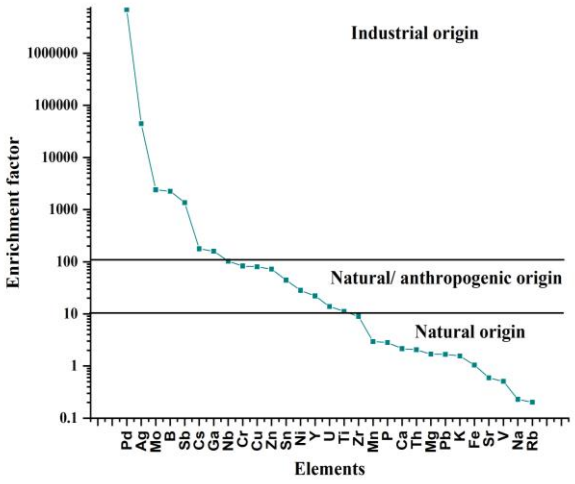

Figure 3. Enrichment Factor (EF) of Metals in PM_{10}

The Enrichment Factor (EF) concept serves as a valuable tool in discerning between natural and human-induced sources of elements. EF values below 5 typically indicate a predominant natural or crustal origin, while values ranging from 5 to 10 suggest a blend of natural and anthropogenic sources. When EF values exceed 10, it points towards primarily anthropogenic origins, often linked to human activities [22, 60]. In this study, the analysis reveals those metals such as Rb, Na, V, Sr, Fe, K, Pb, Mg, Th, Ca, P, and Mn exhibit EF values below 5, indicating their likely derivation from natural crustal sources. Conversely, elements like Zr and Ti display EF values between 5 and 10, implying a combination of natural processes and human activities, such as combustion, construction, or demolition. Finally, elements including U, Y, Ni, Sn, Zn, Cu, Cr, Nb, Ga, Cs, Sb, B, Mo, Ag, and Pd exhibit EF values surpassing 10, strongly indicating their predominantly anthropogenic origin, likely originating from industrial emissions (Fig. 3).

3.2. Source Apportionment and Source Region: In the extensive 2021 investigation in Nainital, Positive Matrix Factorization (PMF 5.0 version) was applied to analyze PM_{10}. A six-factor solution was deemed the most reliable, involving 22 species (OC, EC, WSOC, B, Na, Mg, Al, P, S, Cl, K, Ca, Ti, Cr, Mn, Fe, Ni, Cu, Zn, Ga, Zr, and Mo) and 40 PM_{10} samples. To enhance the model's robustness, Mn, Ga, and Mo were considered weak species, and an extra 10% modelling uncertainty was applied. The PMF analysis results, including source profiles and percentage contributions, are presented in Fig. 4 and Fig. 5 respectively.

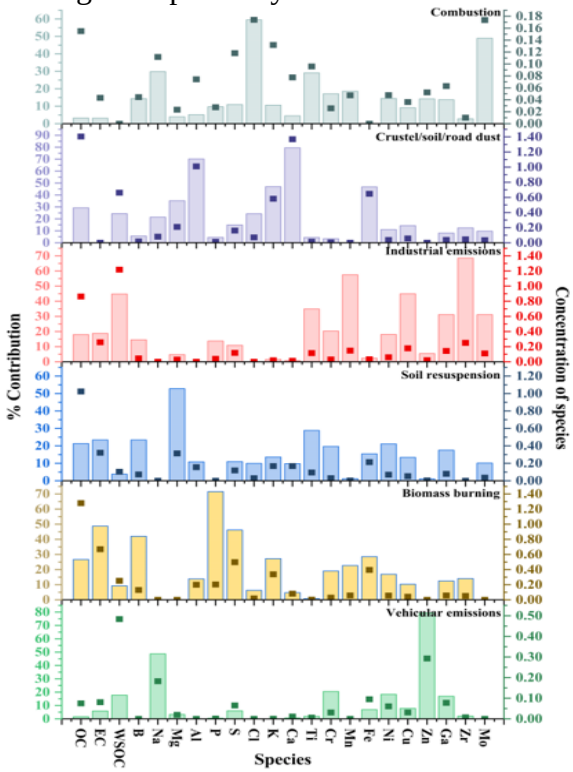

Figure 4: PMF source profile of PM_{10} at Nainital

The identified factors for PM_{10} included two dust-related factors (crustal/soil/road dust and soil resuspension), combustion, vehicular emissions, biomass burning, and industrial emissions.

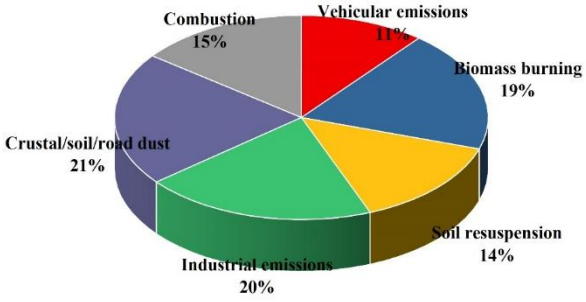

Figure 5: Percentage contribution of the sources extracted by PMF of PM_{10}

Crustal/soil/road dust and soil resuspension factors explained 88% of Mg, indicating a significant influence of soil dust, possibly exacerbated by the tourist-heavy traffic

causing road wear [37-45]. Generally, Ca and Mg are frequently associated with mineral dust and construction activities [25, 46-48]. Given that the sampling site is a tourist hotspot susceptible to the wear and tear of asphalt and concrete roads, primarily due to heavy traffic influence, the increased proportion of crustal elements like Ca and Mg in road dust may result from extensive asphalt and concrete use in road construction [49]. Several other researchers have cited these elements (Ca, Na, Mg, K, and Al) as indicative of a soil dust source in various studies [37-41]. In India, a comprehensive set of marker elements for identifying soil dust includes Al, Si, Ca, Ti, Fe, Pb, Cu, Cr, Ni, Co, and Mn, as discussed in previous studies [42-44]. Combustion, representing 15% of PM_{10} mass, exhibited high loadings for Cl and Mo, suggesting contributions from coal combustion and industrial activities. Cl is emitted through traffic emissions, predominantly from fuel combustion, and is also a significant contributor to coal combustion [50, 51], Vehicular emissions, contributing 13%, displayed elevated Na and Zn loadings, indicative of both exhaust and non-exhaust sources such as brake and tire wear [32, 39, 50, 52, 53]. The elements Na, Cu, Zn, and Ca mostly emitted through vehicular exhaustion as these metals are used as additives in motor oil and fuel [37, 51]. Biomass burning contributed 23%, marked by higher loadings for EC, B, P, and S, linked to agricultural residue burning in the nearby Indo-Gangetic plain [18, 54-58]. Also, there were various forest fire events that took place near sampling site, that could also contribute to the biomass burning source. Biomass burning, whether from agricultural residue burning or forest fires, can release phosphorus into the atmosphere. Plant materials contain phosphorus, and when burned, it can be emitted as PM [56-58]. Industrial emissions, characterized by heightened WSOC, Ti, Mn, Cu, Ga, Zr, and Mo, contributed 22% to the PM_{10} mass [43, 59]. A suite of tracer species, including Ni, Cr, Co, Ga, Cd, Zn, As, Pb, Fe, Cu, Mn, S, and Mo, has been employed in India to discern specific industrial emissions [28, 37, 43, 59].

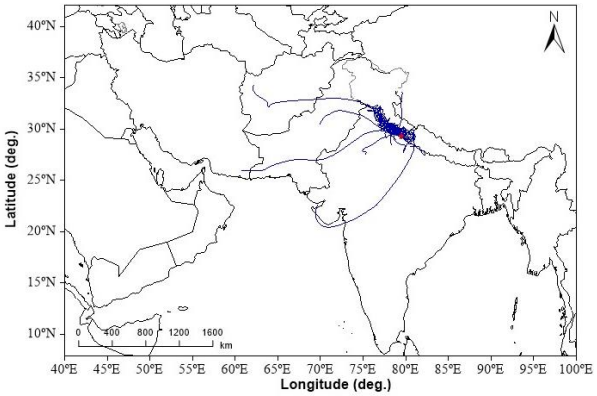

Figure 5: 72 hrs. air mass backward trajectory of PM_{10} at height 500 m above ground level (AGL) at Nainital

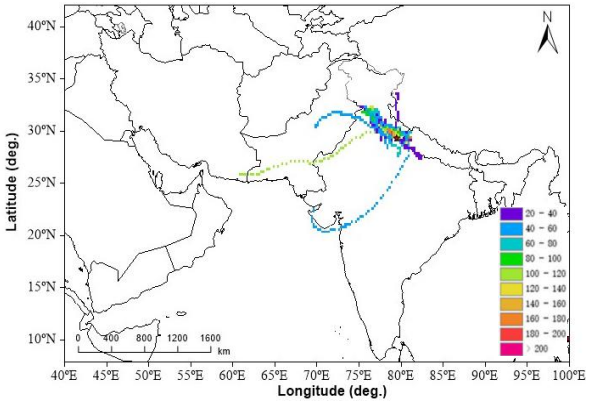

Figure 6. Annual Concentration Weighted Trajectory (CWT) of PM_{10} over Nainital

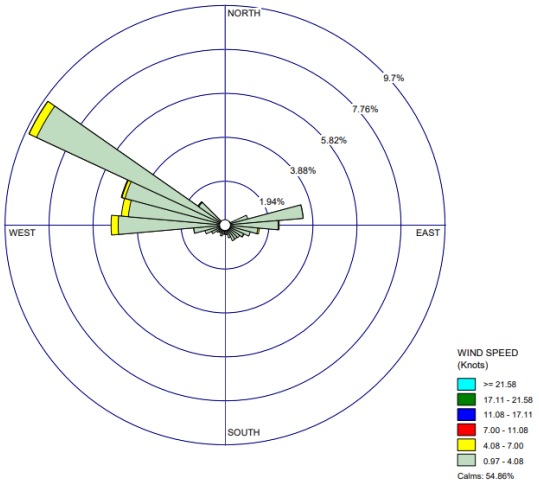

Figure 7: Wind Direction Distribution at Nainital

To comprehend the 72 h. backward trajectories of particulate air masses reaching the sampling site in Nainital, annual trajectories at 500

meters above ground level (AGL) were generated (Fig. 6). Trajectory analysis revealed both local and transboundary origins of PM_{10}, including contributions from northern states, the Thar Desert, and neighboring countries like Pakistan, Afghanistan, Iran, and Nepal [15, 21]. Based on the CWT plot (Fig. 7), it is evident that higher concentrations of PM_{10} (120-180 µg m^{-3}) stem from local emissions. Concentrations ranging between 100-120 µg m^{-3}, originating from regional states within the Indo-Gangetic Plain (IGP) and transboundary regions like Pakistan and Iran, are notable. Additionally, concentrations ranging from 60-80 µg m^{-3} are also attributed to local sources. Lower concentrations (20-60 µg m^{-3}) are observed from local sources, as well as from regional contributors such as Uttar Pradesh, Madhya Pradesh, Maharashtra, North-western regions, and certain northern regions. Furthermore, contributions from the Arabian Sea and transboundary contributors like Pakistan are discernible in this range. Fig. 8 depicts that the predominant wind contribution originated from the northwest, west, northeast, and east directions locally at the sampling site. Locations such as Nainital bus stop and Mall Road are positioned in the northwest direction from ARIES, suggesting their potential contribution to pollution levels at the study site. This observation underscores the significance of these areas as potential sources of pollutants affecting the study site.

3.3. Health Risk Assessment: Fig. 9 presents the evaluation of EC, HQ, and CR for seven heavy elements (Al, Pb, Cr, Mn, Cu, Zn, and Ni) in both adults and children. Notably, HQ values for Cr and Mn in children, reaching 2.33 and 2.99, respectively, exceeded the acceptable limit of 1, indicating a non-carcinogenic health risk. Similarly, in adults, the HQ value for Mn at 1.28 surpassed the safe limit, suggesting a non-carcinogenic health risk as well. Furthermore, adults exposed to Cr may face a potential carcinogenic risk, as its values exceeded the permissible limit of 10^{-4}. Both Cr and Mn are associated with non-exhaust traffic emissions such as tire or brake wear [25, 27, 53]. Conversely, Al, Pb, Cu, Zn, and Ni exhibited HQ values within the permissible limits recommended by USEPA, indicating no health hazards associated with these elements. Prakash et al., 2018 explored the carcinogenic risk in Delhi and identified notably increased health risks linked to $PM_{1.0}$-bound metals, especially for Cr and Ni. The reported risks surpassed safe thresholds for children and approached tolerable limits for adults.

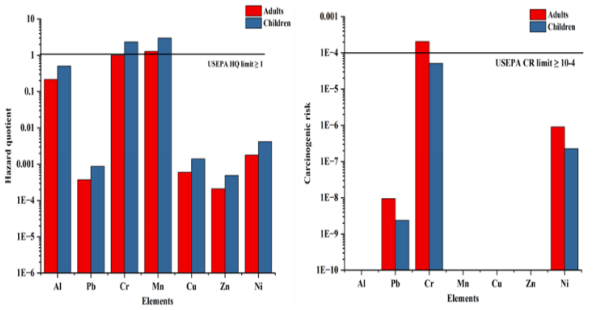

Figure 9: Annual assessment of Hazard Quotient (HQ), and Carcinogenic Risk (CR) of heavy elements on human health

4. Conclusions: In the extensive 2021 study conducted in Nainital, a thorough analysis of PM_{10}, carbonaceous aerosols, and elemental compositions was carried out. The study included assessments of annual concentration averages, Positive Matrix Factorization (PMF)-guided source apportionment, and a health risk evaluation for heavy elements. The average annual PM_{10} concentration stood at 64±6 µg m^{-3}. Carbonaceous aerosols, encompassing OC, EC, WSOC, and SOC, exhibited annual averages of 9.32±0.82 µg m^{-3}, with individual components recording concentrations of 4.90±0.45 µg m^{-3}, 1.48±0.12 µg m^{-3}, 2.72±0.19 µg m^{-3}, and 2.97±0.45 µg m^{-3}, respectively. The elemental composition, constituting about 16% of the total PM_{10} mass, highlighted major contributors like Ca, Al, Fe, S, and K, along with trace levels of various elements (Mg, Pd, B, Mo, Zn, Ag, Nb, Ga, Cl, Ti, Zr, Na, and Cr). Source apportionment identified six primary contributors to PM_{10}, including crustal/soil/road dust, soil resuspension, combustion, vehicular emissions, industrial emissions, and biomass burning. Trajectory analysis unveiled transboundary origins of PM_{10}, originating both locally and from northern Indian states,

the Thar Desert, and the Indo-Gangetic Plain. Substantial contributions were also traced back to neighboring countries, such as Pakistan, Afghanistan, Iran, and Nepal. The main wind contribution originates locally from the northwest, west, northeast, and east directions at the sampling site. Nainital bus stop and Mall Road, situated northwest of ARIES, likely contribute to pollution levels at the study site, highlighting their importance as potential pollution sources. The health risk assessment indicated elevated Hazard Quotient (HQ) values for Cr and Mn in children, signaling a non-carcinogenic health risk. Adults exposed to high Cr levels may face potential carcinogenic risks, while elements like Al, Pb, Cu, Zn, and Ni pose no health hazards, aligning with USEPA guidelines. These insights play a pivotal role in shaping public health policies and strategies to mitigate air pollution-related health risks, providing valuable input for policymakers working to enhance ambient air quality and safeguard human health, especially in higher-altitude regions like Nainital.

Acknowledgments: The authors are thankful to the Director, CSIR-NPL, New Delhi and Head, Environmental Sciences & Biomedical Metrology Division, CSIR-NPL, New Delhi for their encouragement and support of this study. Department of Science and Technology, New Delhi is also thankful for financial support.

Conflict of Interest: Authors declare No conflicts of interest.

References:

[1] S. Fuzzi, U. Baltensperger, K. Carslaw, S. Decesari, H. Denier van der Gon, M. C. Facchini, D. Fowler, I. Koren, B. Langford, U. Lohmann, E. Nemitz, S. Pandis, I. Riipinen, Y. Rudich, M. Schaap, J. G. Slowik, D. V. Spracklen, E. Vignati, M. Wild, M. Williams, and S. Gilardoni, Particulate matter, air quality and climate: lessons learned and future needs, Atmos. Chem. Phys., 15, 2015, 8217–8299.

[2] T.C. Bond, S.J. Doherty, D.W. Fahey, *et al*, Bounding the role of black carbon in the climate system: a scientific assessment, J. Geophys. Res. Atmos., 118, 2013, 5380–5552.

[3] S.K. Sharma, N. Choudhary, P. Srivastava, M. Naja, N. Vijayan, G. Kotnala, T.K. Mandal, Variation of carbonaceous species and trace elements in PM_{10} at a mountain site in the central Himalayan region of India, J. Atmos. Chem., 77, 2020, 1–14.

[4] A.K. Srivastava, K. Ram, P. Pant, P. Hegde, J. Hema, Black carbon aerosols over Manora Peak in the Indian Himalayan foothills: implications for climate forcing, Environ. Res. Lett., 7(1), 2012, 014002.

[5] C. Venkataraman, G. Habib, A. Eiguren-Fernandez, A.H. Miguel, S.K. Friedlander, Residential biofuel in South Asia: Carbonaceous aerosol emissions and climate impacts, Science 307(5714), 2005, 1454–1456.

[6] A. Kumar, A.K. Attri, Biomass combustion a dominant source of carbonaceous aerosols in the ambient environment of western Himalayas, Aerosol Air Qual. Res., 16(3), 2016, 519–529.

[7] Shivani, R. Gadi, R. Kumar, M. Sharma, S.K. Sharma, *et al*, Levels and Sources of organic compounds in Fine Particulate Matter ($PM_{2.5}$) over Delhi and National Capital Region of India, Environ. Sci. Pollut. Res. 25(31), 2018, 31071–31090.

[8] Shivani, R. Gadi, M. Saxena, S.K. Sharma, T.K. Mandal, Short Term Degradation of Air Quality during Major Firework Events in Delhi, India, Meteoro. Atmos. Phys., 131(4), 2019, 753–764.

[9] Shivani, R. Gadi, S.K. Sharma, T.K. Mandal, Seasonal variation, source apportionment and source attributed health risk of carbonaceous aerosols in fine particulate matter over National Capital Region, India, Chemosphere 237, 2019, 124500.

[10] R. Gadi, Shivani, S.K. Sharma, T.K. Mandal, Source apportionment and health risk assessment of organic constituents in fine ambient aerosols ($PM_{2.5}$): a complete year study over National Capital Region of India, Chemosphere, 221, 2019, 583–596.

[11] J.S. Lighty, J.M. Veranth, A.F. Sarofim, Combustion aerosols: factors governing their size and composition implications to human

health, J. Air Waste Manag. Assoc., 50(9), 2000, 1565–1618.
[12] C.A. Pope, M. Ezzati, D.W. Dockery, Fine-particulate air pollution and life expectancy in the United States, New England Journal of Medicine. 360(4), 2009, 376–386.
[13] K. Gajananda, J.C. Kuniyal, G.A. Momin, P.S.P. Rao, P.D. Safai, S. Tiwari, K. Ali, Trend of atmospheric aerosols over the north northwestern Himalayan region, India, Atmos. Environ. 39, 2005,4817–4825.
[14] R. Sheoran, U.C. Dumka, D.G. Kaskaoutis, G. Grivas, *et al*, Chemical composition and source apportionment of total suspended particulate in the central Himalayan region, Atmosphere, 12, 2021, 1128.
[15] N. Choudhary, P. Srivastava, M. Dutta, S. Mukherjee, A. Rai, *et al*, Seasonal Characteristics, Sources and Pollution Pathways of PM_{10} at High Altitudes Himalayas of India, Aerosol Air Qual. Res., 22(7), 2022.
[16] N. Choudhary, A. Rai, J.C. Kuniyal, P. Srivastava, R. Lata, *et al*, Chemical Characterization and Source Apportionment of PM_{10} Using Receptor Models over the Himalayan Region of India, Atmosphere, 14(5), 2023, 880.
[17] R.K. Singh, Assessment of Ambient Air Pollution and Mitigation Strategies towards Achieving Air Quality Index (AQI) in the Indian Himalayan Region, Int. J. Sci. Res, 9(12), 2019.
[18] K. Ram, M.M. Sarin, Spatio-Temporal Variability in Atmospheric Abundances of EC, OC and WSOC over Northern India, J. Aerosol Sci., 41, 2010, 88–98.
[19] P. Hegde, K. Kawamura, H. Joshi, M. Naja, Organic and inorganic components of aerosols over the central Himalayas: winter and summer variations in stable carbon and nitrogen isotopic composition, Environ. Sci. Poll. Res., 23, 2016, 6102–6118.
[20] J. Chow, J. Watson, L.W.A. Chen, W. Arnott, H. Moosmuller, K. Fung, Equivalence of elemental carbon by thermal/optical reflectance and transmittance with different temperature protocols, Environ. Sci. Technol., 38, 2004, 4414–4422.
[21] S.K. Sharma, S. Mukherjee, N. Choudhary, A. Rai, A. Ghosh, *et al*, Seasonal variation and sources of carbonaceous species and elements in $PM_{2.5}$ and PM_{10} over the eastern Himalaya, Environ. Sci. Pollut. Res., 28, 2021, 51642–51656.
[22] S.K. Sharma, T.K. Mandal, M. Saxena, A. Sharma, A. Datta, T. Saud, Variation of OC, EC, WSIC and trace metals of PM10 in Delhi, India. J Atmos Solar-Terres Phys 113, 2014, 10–22.
[23] S. Gupta, S. Shankar, J. C. Kuniyal, et al., Identification of sources of coarse mode aerosol particles (PM_{10}) using ATR-FTIR and SEM-EDX spectroscopy over the Himalayan Region of India. Environ. Sci. Pollut. Res. **31**, 2024, 15788–15808.
[24] R.K. Hooda, N. Kivekäs, M. C. Coen, P. Pietikäinen, V. Vakkari, J. Backman, S.V. Henriksson, E. Asmi, M. Komppula, H. Korhonen, P. Hyvärinen, H. Lihavainen, Driving Factors of Aerosol Properties Over the Foothills of Central Himalayas Based on 8.5 Years Continuous Measurements. Journal of Geophysical Research: Atmospheres, 123(23), 2018, 13,421-13,442.
[25] A. Rai, S. Mukherjee, A. Chatterjee, N. Choudhary, G. Kotnala, T.K. Mandal, S.K. Sharma, Seasonal variation of OC, EC, and WSOC of PM_{10} and their cwt Analysis over the eastern Himalaya, Aerosol Sci. Eng., 4, 2020, 26–40.
[26] M. Mishra, U.C. Kulshrestha, Source impact analysis using char-EC/Soot-EC ratios in the central Indo-Gangetic Plain (IGP) of India, Aerosol Air Qual. Res., 21, 2021, 200628.
[27] M. F. D. Gianini, A. Fischer, R. Gehrig, A. Ulrich, A. Wichser, C. Piot, J.L. Besombes, C. Hueglin, Comparative source apportionment of PM_{10} in Switzerland for 2008/2009 and 1998/1999 by positive matrix factorisation, Atmos. Environ., 54, 2012, 149–158.
[28] Y. Li, B. Liu, Z. Xue, Y. Zhang, X. Sun, C. Song, *et al*, Chemical characteristics and source apportionment of $PM_{2.5}$ using PMF modelling coupled with 1-hr resolution online air pollutant dataset for Linfen, China, Environmental Pollution, 263(B), 2020, 114532.

[29] P. Rai, J.G. Slowik, M. Furger, I. El-Haddad, S. Visser, highly time-resolved measurements of element concentrations in PM_{10} and $PM_{2.5}$: Comparison of Delhi, Beijing, London, and Karakow, Atmos. Chem. Phys., 21, 2021, 717-730.
[30] R. Banoo, S. Gupta, R. Gadi, *et al.* Chemical characteristics, morphology and source apportionment of PM_{10} over National Capital Region (NCR) of India, Environ. Monit. Assess., 196, 2024, 163.
[31] N. Zheng, J. Liu, Q. Wang, Z. Liang, Science of the total environment health risk assessment of heavy metal exposure to street dust in the zinc smelting district, Northeast of China, 408(4),2010, 726–733.
[32] J. Prakash, T. Lohia, A.K. Mandariya, G. Habib, T. Gupta, S.K. Gupta, Chemical characterization and quantitative assessment of source-specific health risk of trace metals in $PM_{1.0}$ at a road site of Delhi, India, Environ. Sci. Pollut. Res., 25, 2018, 8747–8764.
[33] S. Gupta, S.K. Sharma, T.K. Mandal, Elemental Analysis and Health Risk Assessment of $PM_{2.5}$ at an Urban Site of Delhi, Chapter 16, Recent Advances in Metrology, Sanjay Yadav, Naveen Garg, Shankar G. Aggarwal, Shiv Kumar Jaiswal, Harish Kumar, Venu Gopal Achanta, Springer Science and Business Media, 2023.
[34] D. Sah, P.K. Verma, K.M. Kumari, A. Lakhani, Characterisation, Sources and Health Risk of Heavy Metals in $PM_{2.5}$ in Agra, India, Exposure and Health, 49, 2022, 10147.
[35] Q. Zhang, D.R. Worsnop, M.R. Canangaratna, J.L. Jimenez, Hydrocarbon-like and oxygenated organic aerosols in Pittsburgh: Insights into sources and processes of organic aerosol, Atmos. Chem. Phys., 5, 2005, 3289–3311.
[36] A. Chatterjee, S. Mukherjee, M. Dutta, A. Ghosh, S.K. Ghosh, A. Roy, High rise in carbonaceous aerosols under very low anthropogenic emissions over eastern Himalaya, India: Impact of lockdown for COVID-19 outbreak, Atmos. Environ., 244, 2021, 117947.
[37] B. Gugamsetty, H. Wei, C.N. Liu, A. Awasthi, S.C. Hsu, *et al,* Source Characterization and Apportionment of PM_{10}, $PM_{2.5}$ and PM_{1} by Using Positive Matrix Factorization, Aerosol Air Qual. Res., 12, 2012, 476-491.
[38] A. Waked, O. Favez, L.Y. Alleman, C. Piot, J.E. Petit, *et al,* Source apportionment of PM_{10} in a north-western Europe regional urban background site (Lens, France) using positive matrix factorization and including primary biogenic emissions, Atmos. Chem. Phys., 14, 2014, 3325–3346.
[39] M.F. Khan, M.T. Latif, W.H. Saw, N. Amil, M.S.M. Nadzir, M. Sahani, N.M. Tahir, J.X. Chung, Fine particulate matter in the tropical environment: monsoonal effects, source apportionment, and health risk assessment, Atmos. Chem. Phys., 16, 2016, 597–617.
[40] J.H. Jeong, Z.H. Shon, M. Kang, S.K. Song, Y.K. Kim, J. Park, H. Kim. Comparison of source apportionment of $PM_{2.5}$ using receptor models in the main hub port city of East Asia: Busan, Atmospheric Environment, 148, 2017, 115-127.
[41] M. Manousakas, M. Furger, K.R. Daellenbach, F. Canonaco, G. Chen, A. Tobler, P. Rai, *et al,* Source identification of the elemental fraction of particulate matter using size segregated, highly time-resolved data and an optimized source apportionment approach, Atmospheric Environment X, 14, 2022, 100165.
[42] I. Gupta, A. Salunkhe, R. Kumar, Source Apportionment of PM_{10} by Positive Matrix Factorization in Urban Area of Mumbai, India, The Scientific World Journal, 2012, 585791.
[43] T. Banerjee, V. Murari, M. Kumar, M.P. Raju, Source apportionment of airborne particulates through receptor modelling: Indian scenario, Atmos. Res., 164, 2015, 167–187.
[44] S. Jain, S.K. Sharma, N. Choudhary, R. Masiwal, M. Saxena, *et al*, Chemical characteristics and source apportionment of $PM_{2.5}$ using PCA/APCS, UNMIX and PMF at an urban site of Delhi, India, Environ. Sci. Pollut. Res. 24, 2017, 14637-14656.
[45] S.K. Sharma, T.K. Mandal, M.K. Srivastava, *et al*, Spatio-temporal variation in chemical characteristics of PM_{10} over Indo

Gangetic Plain of India, Environ. Sci. Pollut. Res. 23, 2016, 18809–18822.
[46] N. Bukowiecki, P. Lienemann, M. Hill, M. Furger, A. Richard, F. Amato, A.S.H. Prevot, U. Baltensperger, B. Buchmann, R. Gehrig, PM_{10} emission factors for non-exhaust particles generated by road traffic in an urban street canyon and along a freeway in Switzerland, Atmos. Environ., 44, 2010, 2330-2340.
[47] L.R. Crilley, F. Lucarelli, W.J. Bloss, R.M. Harrison, D.C. Beddows, G. Calzolai, S. Nava, G. Valli, V. Bernardoni, R. Vecchi, Source apportionment of fine and coarse par ticles at a roadside and urban background site in London during the 2012 summer Clear fLo campaign, Environ. Pollut., 220, 2016, 766–778.
[48] W. Maenhaut, Source apportionment revisited for long-term measurements of fine aerosol trace elements at two locations in southern Norway, Nucl. Instrum. Meth. B, 417, 2017, 133–138.
[49] D. Fullova, D. Durcanska, J. Hegrova, Particulate matter mass concentrations produced from pavement surface abrasion, MATEC Web Conf., 117, 2017, 00048.
[50] N. Jiang, Q. Li, F. Su, Q. Wang, X. Yu, P. Kang, R. Zhang, X. Tang. Chemical characteristics and source apportionment of $PM_{2.5}$ between heavily polluted days and other days in Zhengzhou, China, Journal of Environmental Sciences, 66, 2018, 188-198.
[51] Q. Dai, B. Liu, X. Bi, J. Wu, D. Liang, Y. Zhang, Y. Feng, P.K. Hopke, Dispersion normalized PMF provides insights into the significant changes in source contributions to $PM_{2.5}$ after the COVID-19 outbreak, Environ Sci. Technol., 54 (16), 2020, 9917-9927.
[52] T. Grigoratos, G. Martini, Brake wear particle emissions: a review, Environ. Sci. Pollut. Res., 22, 2015, 2491–2504.
[53] A. Roy, M. Mandal, S. Das, M. Kumar, R. Popek, A. Awasthi, *et al*, Non-exhaust particulate pollution in Asian countries: A comprehensive review of sources, composition, and health effects, Environmental Engineering Research, 29(3), 2024.
[54] A. Singhal, G. Habib, R.S. Raman, T. Gupta, Chemical characterization of $PM_{1.0}$ aerosol in Delhi and source apportionment using positive matrix factorization, Environ. Sci. Pollut. Res. 24, 2017, 445 – 462.
[55] S. Jain, S.K. Sharma, M.K. Srivastava, *et al*, Source Apportionment of PM_{10} Over Three Tropical Urban Atmospheres at Indo-Gangetic Plain of India: An Approach Using Different Receptor Models, Arch. Environ. Contam. Toxicol. 76, 2019, 114–128.
[56] S.K. Akagi, R.J. Yokelson, C. Wiedinmyer, M.J. Alvarado, J.S. Reid, *et al*, Emission factors for open and domestic biomass burning for use in atmospheric models, Atmos. Chem. Phys., 11, 2011, 4039–4072.
[57] S. Bhuvaneshwari, H. Hettiarachchi, J.N. Meegoda, Crop Residue Burning in India: Policy Challenges and Potential Solutions, Int. J. Environ. Res. Public Health, 16, 2019, 832.
[58] Y. Meng, R. Li, L. Cui, Z. Wang, H. Fu, Phosphorus emission from open burning of major crop residues in China, Chemosphere, 288, 2022, 132568.
[59] S.K. Sharma, T.K. Mandal, M. Saxena, A. Sharma, R. Gautam, Source apportionment of PM_{10} by using positive matrix factorization at an urban site of Delhi, India, Urban Climate, 10, 2014, 656–670.
[60] M.I.C. Abdullah, A.S.R.M. Sah, H. Haris, Geo-accumulation Index and Enrichment Factor of Arsenic in Surface Sediment of Bukit Merah Reservoir, Malaysia, Trop. Life Sci. Res. 31(3), 2020, 109-125.